



Topological Shape Optimization Based on Harmony Search Method

Seung-Min Lee^a, Seog-Young Han^{a*}^a School of Mechanical Engineering, Hanyang University, 222, Wangsimni-ro, Seongdong-gu, Seoul 04763, Korea

ARTICLE INFO

Article history:

Received	3	April	2018
Revised	1	June	2018
Accepted	3	August	2018

Keywords:

Harmony search
Shape optimization
Topological shape optimization
Boundary element index
Boundary elements

ABSTRACT

A new topological shape optimization scheme based on the harmony search (HS) method is proposed, which provides an optimized structural shape for topology and shape optimization simultaneously via shape optimization only. The parameters of the HS method such as harmony memory considering rate, pitch adjusting rate, and band width for topological shape optimization are suggested. Additionally, new schemes such as boundary element index and pitch control number for more stable and robust optimized shape are implemented, and the results of the proposed algorithm are compared with those of the discrete level set method (LSM) for some numerical examples to verify the effectiveness and applicability. From these results, it is shown that objective values and optimized topological shape of the proposed algorithm are similar and convergence rate is improved at least 42% compared to those of the discrete LSM.

1. Introduction

To date, various shape optimization methods have been developed to provide low costs and high efficiency in optimum structural design. Most optimization methods gradually and iteratively modify the present design and produce a new shape based on the previous shape^[1]. Such methods require an effective computation time to perform the iterative structural optimization.

Boundary variation methods for shape optimization were actively studied in the 1980's. Pironneau^[2] suggested mesh moving algorithms, where the design variables are used as coordinates for the nodal points in a finite element model. Kikuchi et al.^[3] verified the significance of regularity in the finite element model in producing a physically optimized shape. Botkin and Bennett^[4] and Braibant and Fleury^[5] proposed a boundary variation method, using a set of

segments such as straight lines, circular and elliptic arcs, and spline curves. Also, although mathematical fundamentals of boundary variation methods have been sufficiently examined for shape optimization and sensitivity analysis, they can be applied to shape optimization when the initial topology is fixed during the iterative optimization. As a result, it is impossible to simultaneously obtain the optimal topology and shape of a structure^[1].

Therefore, shape optimization problems have to be transformed to material distribution problems. Homogenization^[6] and a solid microstructure with a penalization method (SIMP)^[7] were developed in the 1980's, and these techniques represent a remarkable evolution in structural shape optimization. In addition, evolutionary structural optimization (ESO)^[8,9] and additive ESO^[10] have been developed. These approaches perform optimization by removing and adding elements based on sensitivity numbers. In addition, these

* Corresponding author. Tel.: +82-2-2220-0456

Fax: +82-2-2220-2299

E-mail address: syhan@hanyang.ac.kr (Seog-Young Han).

methods were expanded to a bi-directional ESO (BESO)^[11], which carries out optimization by simultaneously adding and removing elements in each iteration.

Topological shape optimization is an effective optimization that simultaneously performs topology and shape optimization. There are two methods, namely the phase field method (PFM) and the level set theory (LSM). The PFM suggested by Bourdin and Chambolle^[12] established that the boundary where two phases coexist was not divided by a line via mathematical expression, but instead by the regions. Since the LSM for topology optimization was suggested by Sethian and Wiegmann^[13], Wang et al.^[14] proposed a topological shape optimization method based on the LSM. Sethian and Osher^[15] evaluated the sensitivities for the shape and topology based on the Hamilton-Jacobi equation.

However, even though the LSM is a very effective topological shape optimization method, its results are considerably dependent on the initial holes^[16] and weight factor of the topological sensitivity^[17]. It requires a proper number of initial holes and a weight factor to obtain an optimized shape through numerical experiments. In addition, since it is based on mathematical gradient methods, the shape can be changed only on the previous boundaries^[18]. Therefore, it is necessary to develop a better and simpler topological shape optimization technique than the LSM.

It has been proved that the HS algorithm^[19] as a probabilistic search algorithm among non-gradient-based methods has a distinguished optimization capability for various engineering problems^[20-23]. However, the algorithm has been applied only to functional optimization or size optimization for truss dome structures. Even though the HS has been applied to static, dynamic stiffness topology^[24,25] and shape^[26] optimization problems, it has not been applied to topological shape optimization.

In this study, the HS method was applied to shape and topological shape optimization to overcome the weaknesses of gradient-based methods. The proposed topological shape optimization algorithm is suggested to provide topology optimization characteristics by performing only shape optimization via searching for the boundary elements of a temporarily optimized structure at each sub-iteration. The proper parameters of the HS method, such as the HMCR, PAR, and BW for topological shape optimization, were investigated in this parametric study. In addition, new

schemes for a more stable and robust optimized shape were implemented, and the results of the proposed topological shape optimization of numerical examples were compared with those of the discrete LSM^[27] to verify its effectiveness and applicability.

2. Formulation of Topological Shape Optimization

2.1 Formulation

The objective of this study was to obtain an optimized structure having the largest static stiffness satisfying the volume constraint through topological shape optimization. The total strain energy was employed as the objective function. Therefore, the static stiffness optimization for topological shape optimization can be formulated as follows:

$$\begin{aligned} \text{Minimize : } U &= \frac{1}{2} \mathbf{f}^T \mathbf{u} \\ \text{Subjected to : } \mathbf{f} &= \mathbf{K} \mathbf{u} \\ V^* - \sum_{j=1}^n V_j x_j &= 0, x_j = \begin{cases} 1 & \text{if element is solid} \\ x_{min} = 0.001 & \text{if element is void} \end{cases} \end{aligned} \quad (1)$$

where U is the total strain energy, \mathbf{f} is the load vector, \mathbf{u} is the displacement vector, the superscript T represents the transpose of a matrix, \mathbf{K} is the global stiffness matrix, V_j is the volume of each element, V^* is the target volume of the optimized topology, x_j is the density of each element, and the subscript j represents the element number.

2.2 Material interpolation

In order to obtain the solid-void design of an optimized topological shape structure, the following material interpolation method^[11] was applied.

$$E(x_j) = E_1 x_j^p \quad (2)$$

Here, E_1 is the elastic modulus of the solid material and p is the penalty exponent factor.

The global stiffness matrix \mathbf{K} can be expressed by the following equation:

$$\mathbf{K} = \sum_j^n x_j^p \mathbf{K}_j \quad (3)$$

where \mathbf{K}_j is the elemental stiffness matrix of the j th solid

element and n is the number of the total elements.

2.3 Sensitivity number

In this study, the sensitivity number of each element for searching effective elements was calculated by differentiating the total strain energy with respect to the density of each element^[11]. However, since it was verified that the sensitivity number obtained above does not provide a robust topological shape, the harmony rate (HR) update rule was implemented. This rule is similar to the pheromone update rule in ACO^[28] and the waggle index update rule^[29] in ABCA. The HR update rule is a rule that updates the tune information in the present iteration using the amount of the tune information H_j shared on each element in the previous iteration and the present note information, t_j . The HR update rule was defined using the HR update coefficient δ as follows:

$$H_j^{(k)} = \delta \times H_j^{(k-1)} + (1 - \delta) \times t_j^{(k)} \quad (4)$$

where k is the number for the present iteration, H is the matrix of the HR, t_j is each note in the HM, and δ is the HR update coefficient. The HR update rule creates a better harmony note from each note in the previous iteration. The improved sensitivity number is defined using the HR update rule as follows:

$$\alpha_j = \begin{cases} \frac{H_j^p}{2} - u_j^T K_j u_j & (0 < H_{\min} \leq H_j \leq 1) \end{cases} \quad (5)$$

3. Definition of the Boundary Elements

The principal aim of this study was to develop a topological shape optimization scheme that simultaneously provides an optimized structural shape through topology optimization as well as shape optimization by performing shape optimization only. Therefore, the boundary elements of a structure for shape optimization should be defined in the first step. These boundary elements correspond to the searching domain associated with the change of the structural shape during shape optimization. The bold black line in Fig. 1 indicates the surface boundary of the structure at the present iteration. The boundary elements are defined by the elements located on each of the upper and lower layers adjacent to the surface elements of the structure, as shown in Fig. 1. The solid and

void elements are dark grey and white in Fig. 1, respectively, where the boundary elements are bright grey.

The boundary elements can be defined using the boundary element indicator (BEI) described by Eq. (6).

$$BEI_j = \begin{cases} +1 & \text{if it is a boundary element} \\ -1 & \text{if it is not a boundary element} \end{cases} \quad (6)$$

Here, BEI_j is the boundary element indicator of the j th element.

In addition, estimation of each element is needed to select more efficient or significantly contributed elements for shape optimization. The estimation of each element was evaluated by its fitness using Eq. (7), which was calculated by the temporary fitness based on the sensitivity number of Eq. (5) multiplied by BEI_j .

$$fitness_j = BEI_j \times temporary\ fitness_j \quad (7)$$

From the above equation, the boundary elements can be distinguished based on the sign of the $fitness_j$ value. That is, the j th element becomes the boundary element if the sign of $fitness_j$ is positive. Likewise, shape optimization can be carried out by redefining BEI_j for the newly searched boundary elements at each iteration. However, this method cannot naturally produce holes inside the structure. The reason for this is that this method refines BEI_j only once at each iteration, based on the fitness of entire boundary elements at each iteration. Therefore, the boundary shape of the structure can be changed, but holes inside the structure cannot be naturally produced.

Since topology optimization is the best way to reduce structural weight, topology optimization is generally performed first and then, shape optimization follows for the structural

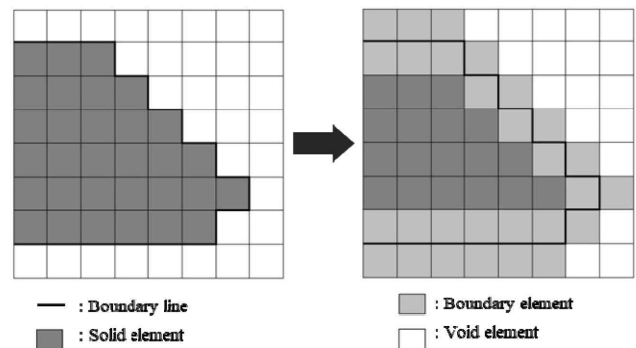


Fig. 1 Definition of the boundary elements

design. In this study, we suggest a shape optimization scheme that simultaneously performs topology and shape optimization only during the shape optimization process. In other words, the proposed algorithm possesses a topology optimization characteristic by continuously reestablishing the BEI for all of the boundary elements whenever an element among them is searched. In this manner, holes inside the structure may be naturally generated.

4. Topological Shape Optimization Using the Harmony Search

4.1 Harmony search

Harmony search (HS) is a search algorithm inspired by the way an orchestra performs as a metaheuristic method. Different from gradient-based methods, it does not require gradient information since it uses only a random and probabilistic search and has a high search capability for a global solution. The optimization process is carried out by estimating and updating each note harmoniously obtained by probabilistically tuning each randomly generated note. Thus, the way an orchestra performs is a search method and each note plays a role as a design variable in the HS algorithm. The number of randomly generated notes in harmony memory (HM) is called the harmony memory size (HMS). A local solution can be avoided by tuning the notes through a probabilistic search using the principal parameters, including the harmony memory considering rate (HMCR) and pitch

adjusting rate (PAR)^[19].

In order to apply the HS method to topological shape optimization, the variables of the method should be properly transformed. The entire search domain corresponds to the boundary elements in topological shape optimization. Each note corresponds to each discretized element in the total design domain. HM is a set of temporary candidate solutions and is composed of solid-void elements. The HMS is set to 1, considering that the finite element analysis has to be carried out as many times as the value of the HMS. Harmonious notes in topological shape optimization correspond to solid elements, such that a set of these indicates a temporary candidate solution. Meanwhile, unharmonious notes correspond to the void elements, such that a set of these indicates a void region in an optimized structure. The correspondences of the variables in the HS method to those in the suggested topological shape optimization based on the proposed method are shown in Table 1.

4.2 Methods for topological shape optimization

A topological shape optimization algorithm using the HS algorithm was developed after verifying that the shape optimization method based on the HS was successfully performed. Since the BEI_i is updated once at each iteration in the shape optimization above, this method can only search the solutions in the boundary elements of the structure; therefore, holes in the structure cannot be created.

In order to create holes naturally and to optimize the

Table 1 Correspondences of the variables in the HS method to those in topological shape optimization using the HS

Harmony search	Topological shape optimization
Search range	Boundary elements domain
Harmony memory (HM)	All elements discretized in full design domain
Quality of each feasible solution	Fitness
Better harmony memory vectors than the worst vector	The number of solid elements corresponding to target volume
The worst vector in HM	Void elements
($\text{rand} \leq \text{HMCR}$) The probability of choosing one value from the historic values stored in the HM	The probability of choosing one value in the HM
($\text{rand} \leq \text{PAR}$) The rate of adjustment for the pitch chosen from the HM	The rate of adjustment for the element position chosen from the HM
($\text{rand} \leq \text{HMCR}$) The probability of randomly choosing one feasible value not limited to those stored in the HM	The probability of choosing one value in the HM
($\text{rand} \leq \text{PAR}$) The rate of doing nothing	The rate of doing nothing

boundary elements simultaneously in topological shape optimization, the BEI_i should be updated continuously whenever a temporary candidate solution in each iteration is found (further explained in Section 4.4). Through the aforementioned process, the solid elements are distributed to efficient regions in the overall design domain, based on fitness values, although only the boundary elements are optimized. When the BEI_i is updated continuously, whenever a temporary candidate solution is found, the locations of the defined boundary elements can be moved sequentially, from the locations of the boundary elements in the initial topology to the locations of the efficient elements in the overall design domain, in each sub-iteration. This results in a continual process of topology optimization, although only a shape optimization based on the HS is performed.

After an approximate structure is created, the locations of the defined boundary elements are almost fixed in each iteration, because it is impossible to create any subsequent new holes in the structure. Hence, shape optimization proceeds after the convergence of an approximate topology of the structure.

In order to secure robustness and fast convergence of the proposed topological shape optimization algorithm, various methods have been applied. A filtering scheme was employed to prevent a checkerboard pattern and a simple average scheme was implemented for stability of the optimization process^[11], as with the shape optimization algorithm. It was found that these two schemes may not successfully provide a satisfactory convergence rate and topological shape.

Thus, newly supplementary methods were employed in the proposed topological shape optimization algorithm. In terms of the number of layers searching for boundary elements, the case with two layers from the boundary of the structure showed a faster convergence rate as well as robust topological shape than that with one layer. In order to avoid a local solution, the pitch control number was applied, which is similar to the limit value suggested by Park and Han^[29]. The pitch control value was in the range of 5-10 and a simple average scheme was not used at every specific iteration number. In cases where the sensitive numbers are very small, an effective search may not be possible. As a result, the sensitive numbers are normalized and then, the fitness for each element is calculated. Also, the proper ranges of the parameters in topological shape optimization were determined

through a parametric study with HMCR, PAR, and BW values of 0.7-0.85, 0.65-0.7, and 30-40, respectively. The HR update coefficient is in the range of 0.7-0.8.

4.3 Topological shape optimization procedure based on HS

Step 1. Initialization

The design domain for topological shape optimization was discretized by a 4-node rectangular finite element. Arbitrary values of the HMCR, PAR, BW, HR update coefficient, pitch control value, and filtering radius were chosen within proper ranges determined by the parametric study.

Step 2. Calculation of fitness

The fitness for each element was calculated based on the sensitivity numbers determined by the temporary fitness from Eq. (5) and the BEI from Eq. (7). In this step, the simple average scheme^[11] and pitch control value are used. The simple average scheme is as follows:

$$\alpha_j^{(k)} = \frac{\alpha_j^{(k-1)} + \alpha_j^{(k)}}{2} \tag{8}$$

Step 3. Generation of a new HM

Temporary candidate solutions, x'_m and h'_m , are randomly selected in the boundary elements. The subscript m indicates the elemental number. The movement of h'_m is dependent on the HMCR in Eq. (9). When rand is smaller than or equal to HMCR, h'_m moves to the PAR procedure. Otherwise, h'_m is randomly reselected in the boundary elements.

$$x'_i = \begin{cases} x'_i \in \{x_i^1, x_i^2, \dots, x_i^{\text{HMS}}\} & (\text{if rand} \leq \text{HMCR}) \\ x'_i \in X_i & (\text{if rand} > \text{HMCR}) \\ \text{rand} = \text{random number between 0 to 1} \\ X_i = \text{possible region of each design variable} \end{cases} \tag{9}$$

The h'_m value moved in the PAR procedure is rearranged due to the PAR in Eq. (10). If rand is smaller than or equal to PAR, h'_m is moved to the adjacent element in the BW range.

$$x'_i = \begin{cases} x'_i \leftarrow x'_i + \gamma & (\text{if rand} \leq \text{PAR}) \\ x'_i & (\text{if rand} > \text{PAR}) \\ \gamma = \text{BW} \times u(-1, 1) \end{cases} \tag{10}$$

Here, BW indicates the arbitrary width with which the

selected element h'_m can be moved, and $u(-1, 1)$ is a random number with a value between -1 and 1.

Step 4. Updating the HM

In this step, whenever the m th temporary candidate solutions, x'_m and h'_m , are being searched, the BEI for the boundary elements defined by Eq. (6) should be continuously redefined. Thus, the element with a better fitness value for the two candidate solutions, x'_m and h'_m , is stored as a solid element and the other is stored as a void element. This procedure is iterated by the number of the total boundary elements and naturally produces holes inside the optimized structure.

Step 5. Control for the target volume

Since the number of the stored solid boundary elements in HM may not satisfy the target volume, the target volume should be satisfied by controlling the number of boundary elements, based on the fitness values.

Step 6. Calculate the objective function value for the updated optimal solution using a four-node rectangular finite element

The objective function value was calculated by using a filtering scheme^[11].

Step 7. Checking convergence

The following convergence criterion of Eq. (11) was applied to terminate the optimization process.

$$error = \frac{\left| \sum_{r=1}^s (U^{(k-r+1)} - U^{(k-s-r+1)}) \right|}{\sum_{r=1}^s U^{(k-r+1)}} \leq \tau \quad (11)$$

Here, τ is the allowable convergence tolerance (0.001), U is the total strain energy, k is the number of the present iteration, and s is the integer number resulting in a converged objective function. In this study, s was selected as 5 to ensure the change of the objective function was sufficiently small over the last 10 iterations. If the convergence criterion is not satisfied, proceed to Step 2 and the above procedure is repeated until the convergence criterion is satisfied.

The flowchart of topological shape optimization based on the HS is shown in Fig. 2.

5. Application Examples

In order to verify the effectiveness of the suggested

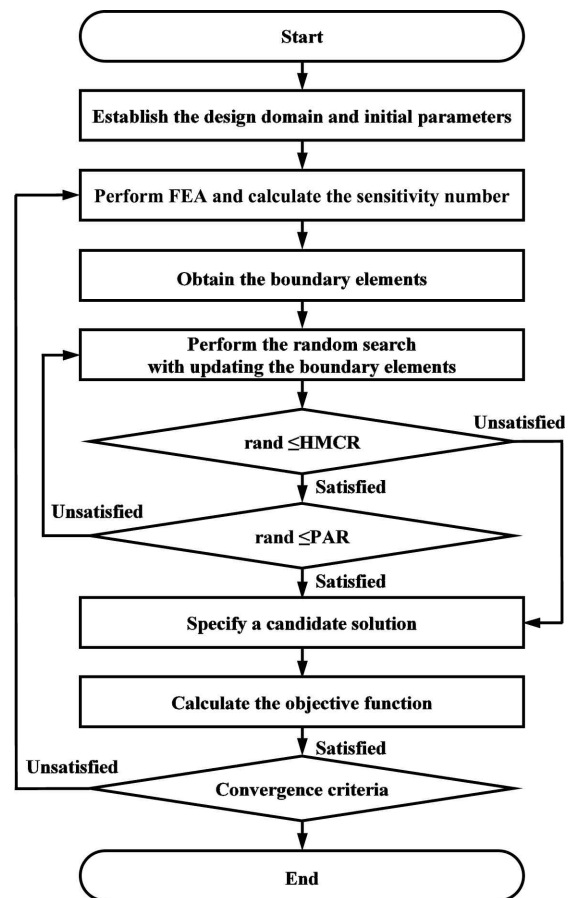


Fig. 2 Flowchart of topological shape optimization using the HS

topological shape optimization scheme based on the HS, three typical examples were investigated. Since the optimization scheme was performed using a four-node rectangular finite element, the optimized shapes were compared with those of the discrete LSM^[27]. The objective of the examples was to obtain an optimized topological shape having the smallest strain energy (the largest static stiffness) under the prescribed volume constraint. The methods and proper parameters of the HS previously mentioned in Section 4.2 were used for the topological shape optimization. The values of HMCR, PAR, and BW were selected to be 0.85, 0.65, and 40, respectively. The penalty exponent factor p was chosen as 3. The number of search boundary lines was two and the HR update coefficient was 0.8. The filtering radius r_{min} and the pitch control were selected as 2.5-4 and 5-10, respectively. The error limit of the convergence criterion was 0.1%. The topological shape optimization based on the HS method was performed 10 times for the three typical examples since the HS is a metaheuristic algorithm.

5.1 A short cantilever beam

The suggested algorithm was applied to topological shape optimization for a short cantilevered beam subjected to a vertical load at the center of the free end, as shown in Fig. 3. The dimensions of the beam are as follows: a length of 0.8 m, a height of 0.6 m, and a thickness of 0.001 m. The vertical load (P) is 100 kN, the Young's modulus is 100 GPa, and the Poisson's ratio is 0.3. The volume constraint is 40% of the initial volume. The design domain was divided into 80×60 four-node rectangular finite elements. The filtering radius r_{min} and the pitch control were selected as 3 and 5, respectively. The linear weight factor in the discrete LSM was 4.

The optimized topological shape and iteration number according to the HS and discrete LSM are shown in Table 2. The methods produce almost the same shapes, but the iteration number of the HS is much smaller than that of the discrete LSM. The iteration histories obtained from the HS and discrete LSM method are shown in Fig. 4. It was verified that the HS method shows fast and stable convergence. The beginning part of optimization in the HS produced very large objective function values. The reason is that the topological shape optimization is performed in a constant volume throughout the optimization process.

The average objective function value and convergence iteration number are 3.102 J and 27.6 for the suggested

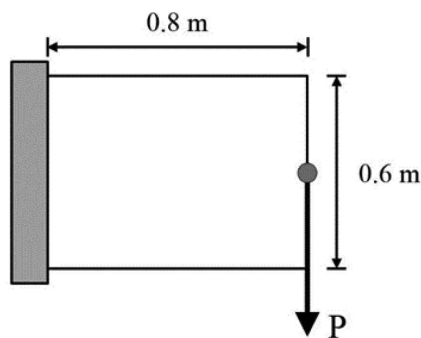
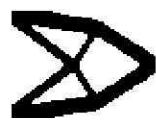



Fig. 3 Problem definition of a short cantilever beam

Table 2 Comparison of optimized topological shapes for the short cantilever beam

Method	Harmony Search	Discrete LSM
Optimized Design (Iteration number)	 (27.6)	 (48)

method and 3.0874 J and 48 for the discrete LSM, respectively. It is known that the convergence rate of the suggested method improved by up to 42% compared to that of the discrete LSM. The standard deviation for the suggested scheme was 0.0079 J, and the robust topologies were obtained for 10 trials.

5.2 A simply supported MBB beam

The suggested algorithm was applied to topological shape optimization for a simply supported MBB beam subjected to a vertical load at the center of the bottom side, as shown in Fig. 5. The dimensions of the beam are as follows: a length of 0.8 m, a height of 0.4 m, and a thickness of 0.001 m. The vertical load (P) is 100 kN, the Young's modulus is 100 GPa, and the Poisson's ratio is 0.3. The volume constraint is 40% of the initial volume. The design domain was divided into 80×40 four-node rectangular finite elements. The radius of the filter scheme r_{min} and the pitch control were chosen as 3 and 10, respectively. The linear weight factor w in the discrete LSM was 4. The optimized shapes from each method are detailed in Table 3.

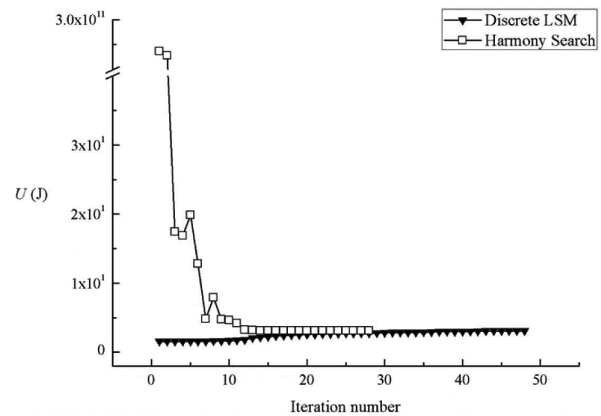


Fig. 4 Iteration history for the objective function value of the short cantilever beam

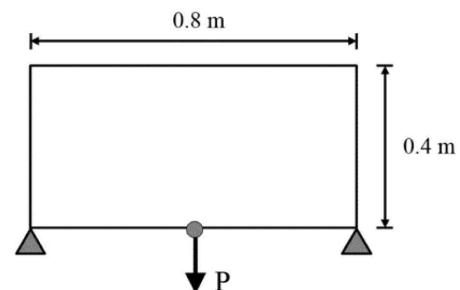




Fig. 5 Problem definition of the simply supported MBB beam

Table 3 Comparison of optimized topological shapes for the simply supported MBB beam

Method	Harmony Search	Discrete LSM
Optimized Design (Iteration number)	 (27.9)	 (63)

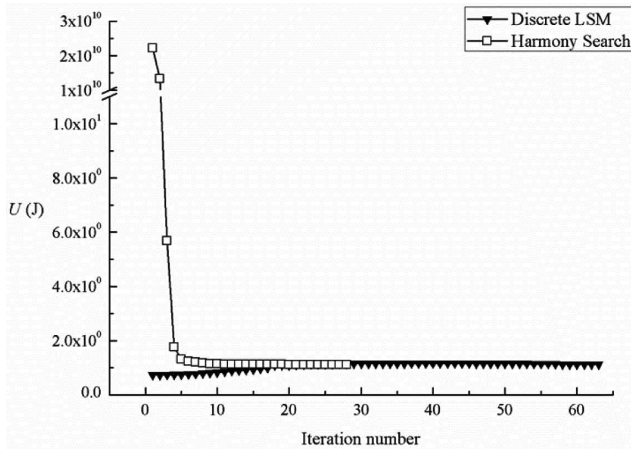


Fig. 6 Iteration history for the objective function value of the simply supported MBB beam

The optimized shape from the suggested topological shape optimization based on the harmony search shows a very similar shape to the shape obtained from the discrete LSM. The average objective function value and convergence iteration number of each method are 1.1172 J and 27.9 for the suggested method and 1.224 J and 63 for the discrete LSM, respectively. Also, it was demonstrated that the convergence rate of the proposed method is much faster than that of the discrete LSM and the iteration history of the suggested scheme is very stable, as shown in Fig. 6. The standard deviation for the suggested scheme was 0.0023 J, and the robust topologies were obtained for 10 trials.

5.3 Knee structure

The suggested algorithm was applied to topological shape optimization for a knee structure subjected to a vertical load at the center of the bottom side, as shown in Fig. 7. The dimensions of the beam are as follows: a length of 0.6 m, a height of 0.6 m, and a thickness of 0.001 m. The vertical load (P) is 100 kN, the Young’s modulus is 100 GPa, and the Poisson’s ratio is 0.3. The volume constraint is 40% of the initial volume. The design domain was divided into 60×60 four-node rectangular finite elements. The radius of the filter scheme r_{min} and pitch control were selected as 3 and 5,

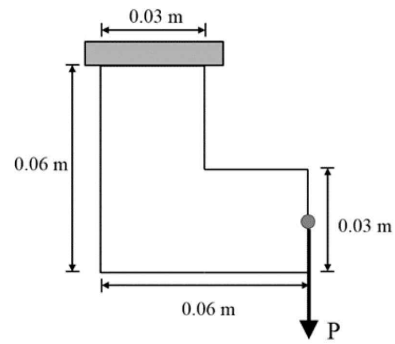




Fig. 7 Problem definition of the knee structure

Table 4 Comparison of optimized topological shapes for the knee structure

Method	Harmony Search	Discrete LSM
Optimized Design (Iteration number)	 (31.8)	 (83)

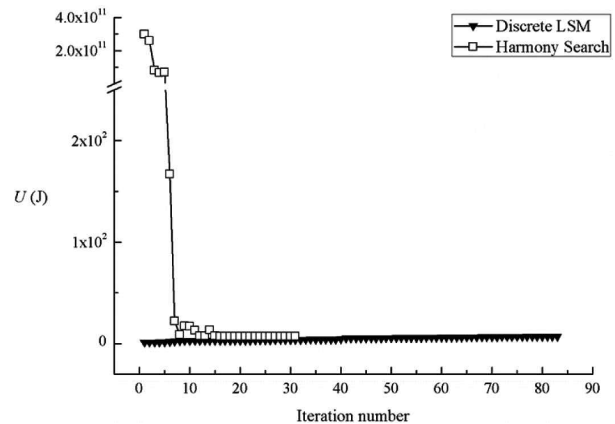


Fig. 8 Iteration history for the objective function value of the knee structure

respectively. The linear weight factor in the discrete LSM was 7. The optimized shape for each method is listed in Table 4.

The optimized shape from the suggested topological shape optimization based on the harmony search for this example also shows a very similar shape as the shape obtained from the discrete LSM. The average objective function value and convergence iteration number due to each method are 6.9795 J and 31.8 for the suggested method and 6.8820 J and 83 for the discrete LSM, respectively. Also, it was demonstrated that the convergence rate of the proposed method is much faster than that of the discrete LSM and the iteration history of the suggested scheme is very stable, as shown in Fig. 8. The standard deviation for the suggested scheme was 0.039 J, and

the robust topologies were obtained for 10 trials.

6. Conclusions

A new topological shape optimization scheme based on the harmony search method is proposed in this paper. The suggested scheme simultaneously performs topology and shape optimization employing only a shape optimization process. In other words, the proposed algorithm has a characteristic of topology optimization in that it continuously reestablishes BEI for all of the boundary elements whenever an element among them is searched. In this manner, holes may be naturally generated inside the structure.

Also, proper ranges of the parameters in the topological shape optimization were determined through a parametric study to produce a proper optimized shape. Various schemes were employed for stability, robustness, and a fast convergence rate. From the above results, the following conclusions can be made.

(1) The harmony search method was properly implemented for the suggested topological shape optimization algorithm. In addition, the various applied schemes provide stability, robustness, and a fast convergence rate.

(2) It was demonstrated that the objective values and optimized topological shape of the proposed algorithm are very similar and the convergence rate was improved by at least 42% compared to those of the discrete level set method.

(3) The effect of topology optimization was realized through the proposed boundary element index (BEI) during only a shape optimization process.

References

- [1] Munk, D. J., Vio, G. A., Steven, G. P., 2015, Topology and Shape Optimization Methods Using Evolutionary Algorithms: A Review, *SMO*, 52:3 613-631.
- [2] Pironneau, O., 1984, *Optimal Shape Design for Elliptic Systems*, Springer, Berlin.
- [3] Kikuchi, N., Chung, K. Y., Torigaki, T., Taylor, J. E., 1986, Adaptive Finite Element Methods for Shape Optimization of Linearly Elastic Structures, *Comput. Methods Appl. Mech. Engrg.*, 57:1 67-91.
- [4] Botkin, M. E., Bennett, J. A., 1985, Shape Optimization of Three Dimensional Folded Shape Structures, *AIAA J.*, 23:11 1804-1810.
- [5] Braibant, V., Fleury, C., 1984, Shape Optimal Designs Using b-splines, *Comput. Methods Appl. Mech. Engrg.*, 44:3 247-267.
- [6] Bendsoe, M. P., Kikuchi, N., 1988, Generating Optimal Topologies in Structural Design Using a Homogenization Method, *Comput. Methods Appl. Mech. Engrg.*, 71:2 197-224.
- [7] Bendsoe, M. P., 1989, Optimal Shape Design as a Material Distribution Problem, *Struct. Multidiscip. Optim.*, 1:4 193-202.
- [8] Li, Q., Steven, G. P., Querin, O. M., Xie, Y. M., 1999, Evolutionary Shape Optimization for Stress Minimization, *Mech. Res. Comm.*, 26:6 657-664.
- [9] Xie, Y. M., Steven, G. P., 1997, *Evolutionary Structural Optimization*, Springer.
- [10] Querin, O. M., Steven, G. P., Xie, Y. M., 2000, Evolutionary Structural Optimisation Using an Additive Algorithm, *Finite. Elem. Anal. Des.*, 34:3-4 291-308.
- [11] Huang, X., Xie, M., 2010, *Evolutionary Topology Optimization of Continuum Structures: Methods and Applications*, John Wiley & Sons.
- [12] Bourdin, B., Chambolle, A., 2003, Design-dependent Loads in Topology Optimization, *ESAIM. COCV.*, 9 19-48.
- [13] Sethian, J. A., Wiegmann, A., 2000, Structural Boundary Design Via Level Set and Immersed Interface Methods, *J. Comput. Phys.*, 163:2 489-528.
- [14] Wang, M. Y., Wang, X., Guo, D., 2003, A Level Set Method for Structural Topology Optimization, *Comput. Methods Appl. Mech. Engrg.*, 192:1-2 227-246.
- [15] Sethian, J. A., Osher, S., 1988, Fronts Propagating with Curvature Dependent Speed: Algorithms Based on Hamilton-Jacobi Formulations, *J. Comput. Phys.*, 79:1 12-49.
- [16] Allaire, G., Jouve, F., Toader, A. M., 2004, Structural Optimization Using Sensitivity Analysis and a Level-set Method, *J. Comput. Phys.*, 194:1 363-393.
- [17] Challis, V. J., 2010, A Discrete Level-set Topology Optimization Code Written in Matlab, *Struct. Multidiscip. Optim.*, 41:3 453-464.
- [18] Sigmund, O., Maute, K., 2013, Topology Optimization Approaches a Comparative Review, *Struct. Multidiscip. Optim.*, 48 1031-1055.
- [19] Geem, Z. W., Kim, J. H., Loganathan, G., 2001, A New Heuristic Optimization Algorithm: Harmony Search, *Simulation*, 76:2 60-68.
- [20] Lee, K. S., Geem, Z. W., 2004, A New Structural Optimization Method Based on The Harmony Search Algorithm, *Comput. Struct.*, 82:9-10 781-798.
- [21] Lee, K. S., Geem, Z. W., 2005, A New Meta-heuristic Algorithm for Continuous Engineering Optimization: Harmony Search Theory and Practice, *Comput. Methods Appl. Mech. Engrg.*, 194:36-38 3902-3933.

- [22] Martini, K., 2011, Harmony Search Method for Multimodal Size, Shape, and Topology Optimization of Structural Frameworks, *J. Struct. Eng.*, 137:11 1332-1339.
- [23] Paik, K., Jeong, J., Kim, J., 2001, Use of a Harmony Search for Optimal Design of Cofferdam Drainage Pipes, *Journal of the Korean Society of Civil Engineers*, 21:2B 119-128.
- [24] Lee, S. M., Han, S. Y., 2014, Topology Optimization Scheme Based on Harmony Search Method, *Proceedings of the KSMTE Autumn Conference*, 98.
- [25] Lee, S. M., Han, S. Y., 2015, Topology Optimization for Dynamic Problem Using Harmony Search, *Proceedings of the KSMTE Spring Conference*, 199.
- [26] Lee, S. M., Han, S. Y., 2015, Shape Optimization Using Harmony Search, *Proceedings of the KSMTE Spring Conference*, 200.
- [27] Challis, V. J., 2010, A Discrete Level-set Topology Optimization Code Written in Matlab, *Struct. Multidiscip. Optim.*, 41:3 453-464.
- [28] Kaveh, A., Hassani, B., Shojaee, S., Tavakkoli, S., 2008, Structural Topology Optimization Using Ant Colony Methodology, *Eng. Struct.*, 30:9 2559-2565.
- [29] Park, J. Y., Han, S. Y., 2013, Swarm Intelligence Topology Optimization Based on Artificial Bee Colony Algorithm, *Int. J. Precis. Eng. Manuf.*, 14:1 115-121.